Journal of Advances in Science and Technology

Vol. 10, Issue No. 21, February-2016, ISSN 2230-9659

CDS QUANTUM DOTS: AQUEOUS SYNTHESIS, SPECTROSCOPIC AND MICROSCOPIC INVESTIGATION

AN INTERNATIONALLY INDEXED PEER REVIEWED & REFEREED JOURNAL

www.ignited.in

Journal of Advances in Science and Technology
Vol. 10, Issue No. 21, February-2016, ISSN 2230-9659

CDS Quantum Dots: Aqueous Synthesis, Spectroscopic and Microscopic Investigation

Mamohan L. Satnami[1] Sandeep Kumar Vaishanav[2] Hitesh K. Dewangan[3] Rekha Nagwanshi[4] Kallol K Ghosh[5]

[1]School of Studies in Chemistry, Pt. Ravi Shankar Shukla University, Raipur (C.G.), 492010, India

[2]Department of Chemistry, Govt. Madhav P.G. Science College Ujjain (M.P.), 456010, India

Abstract – The spherical shape CdS quantum dots with cubic zinc blend phase were synthesized through aqueous route using cadmium chloride and thiourea as cadmium and sulfur source and thioglycolic acid as a stabilizing agent. The size regime of the CdS quantum dots is in between 1.5 to 4.1±0.9 nm. The effect of concentration of cadmium and TGA has been investigated to explain the growth kinetics and stabilization of CdS quantum dots. Structural and morphological studies carried out by X-ray diffraction (XRD), Transmission electron microscopy (TEM), and Scanning electron microscopy (SEM). Optical properties have been studied by UV-visible spectroscopy, Fluorescence measurements, and FTIR analysis. FTIR study suggested the thiolated interaction between CdS and thioglycolic acid. The electronic band gap was found to increase up to 3.93 eV from bulk 2.42 eV. The effect of cationic and anionic surfactants on stabilization of TGA capped CdS quantum dots have been studied. The first order growth kinetic was observed and k_{obs} 5.78x 10^{-4} s^{-1} was obtained in optimized condition.

Key Words: Quantum dot, Electronic Band gap, Surfactant, Growth Kinetics.

----------♦----------

1. INTRODUCTION

Tremendous interest has been growing for Semiconductor quantum dots (QDs) in recent years due to their promising applications in optical devices, solar cells, biosensors, and biological imaging [1–8]. Luminescent QDs possesses many advantages compared to common organic fluorophores such as high photoluminescence (PL), high quantum yield (QY), tunable emission wavelength, multiplexing capabilities, and high photostability against photobleaching. CdS, CdSe, and CdTe that are Group II−VI semiconductor QDs have extensively studied because of the simplicity with which their emission in the visible range can easily tune by changing their diameter and advances in their fabrication methods. CdS is one of the important direct-band semiconductors with a bandgap (Eg) of 2.42 eV. CdS QDs employed for photoelectric conversion in solar cells, in light-emitting diodes (LEDs) for flat-panel displays [9–12] and for biological applications [13, 15]. Unique properties of QDs depend on the diameter, hence controlling size and size distribution as well as crystallinity and surface defects are crucial for tailoring its properties. The properties of such smaller nano-system extremely depend on the confinement of the quasi particles (electrons, holes, and phonons, etc.) down to radii less than 10 nm. The nonlinear optical properties and the quick response time make the quantum confined CdS system tempting for the production of various optoelectronic devices such as solar cells, laser diodes, LEDs, photomultiplier, photoconductors, and wavelength converters. The electron–phonon coupling in CdS is of prime importance because its strength increases with decreasing crystallite size. Compared to the electronic states, there is not much information available on the vibrational modes of nanocrystal CdS quantum dots (QDs) [16]. There are several methods developed for the production of CdS QDs. The organometallic approach and its alternatives, which is based on the high temperature decomposition of organometallic precursors quickly injected in to the well-stirred and hot organic solvents, generally provide the best quality QDs [17-22]. However, for most of the biological applications, the QDs must be soluble in water. Therefore, ligand exchange is a way to achieve water solubility. Small thiol-based molecules generally used to substitute hydrophobic capping agents like trioctylphosphine oxide (TOPO) or long-chain amines used to control the growth process at high temperature. Moreover, some chemicals used in this route are highly toxic, pyrophoric and/or very expensive. Finally, the organometallic approach is extremely inappropriate in terms of scaling up for large-scale industrial

production because of the requirement of high-energy requirement for the synthetic process. In parallel with the success of organic synthetic routes, aqueous routes have also developed to tackle problems associated with phase transfer. The depletion in optical properties (diminishing fluorescence QY and photo stability) could be avoided by direct synthesis in an aqueous medium. In the aqueous synthesis of CdS QDs, small hydrophilic thiols such as thioglycolic acid (TGA), 3-mercaptopropionic acid (MPA), and thioglycerol (TG) are normally used as a surface stabilizing agent, which produce nanomaterial with good emission efficiencies [17, 23–30]. In both the synthetic route, nucleation takes place just after the injection of precursor, and continues until the temperature and the precursor concentration drop below a critical threshold. New synthetic methods that do not require the injection of precursors have also been developed. Some of the reports have been recently published on one-pot non-injection routes to semiconductor nanocrystals either via the organometallic method [31–35], in aqueous solution [36, 37], or under microwave irradiation [38].

Surfactants are amphiphilic molecule which possess a polar head group and nonpolar tail, which forms micelles in the solution which can act as support or template for the growth of smaller moieties i.e. Quantum dots, When micellar solutions are used, the aqueous solution forms a nanoreactor and CdS is present in the core of the micelle [39, 40]. Spherical micelles formed in the aqueous medium. When CTAB used as a capping agent, it results in spherical shapes because the nucleation and growth of the particle occurs in the cavity of the micelle obtained[39, 40]. These micelles have a diameter range in nanometers, so there is possibility that the growing nano-objects can entangle within these vesicles and form a stable dispersion. Despite of high utility of the surfactants in controlling the growth i.e. size and optical properties of metallic nanoparticles, there are very few reports regarding the surfactant mediated assembly of CdS QDs. Therefore, an attempt has been made for studying the effect of surfactant on the stability and growth of CdS quantum dots stabilized by thioglycolic acid in cationic and anionic micellar media.

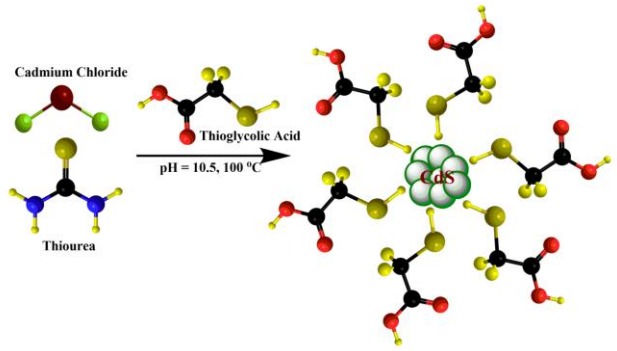

Scheme-1 Cartoon representation of TGA capped CdS QDs synthesis

EXPERIMENTAL SECTION

Materials and Reagent

Cadmium chloride pentahydrate ($CdCl_2.5H_2O$), thioglycoloic acid ($SHCH_2CH_2COOH$), thiourea (NH_2CSNH_2), cetyltrimethyl ammonium bromide (CTAB), sodium dodecyl sulphate (SDS) and sodium chloride (NaCl) were procured from Sigma Aldrich and used without further purification. All the experiments were performed using Millipore water obtained from milliQ system.

2.2 Synthesis of TGA stabilized CdS quantum dots

A 40 mg of cadmium chloride and 22.8 mg of thiourea (TU) dissolved in 30ml of water to prepare Cd^{2+}/thiourea precursor solution. 20ml of thioglycolic acid (TGA) solution containing (30 µl of TGA) then added to the precursor solution and the pH of the reaction mixture adjusted to 10.5 with 1.0 M NaOH (**Scheme-1**). The typical molar ratio of Cd^{2+}: TU: TGA was 1:2:3 in our experiments. The solution was then nitrogen bubbled for 30 minutes and then transferred to three necked round bottom flask, which is connected into the heating mantle with condenser. The completely nitrogen bubbled solution was then set up on the reflux for the nucleation and growth of CdS QDs. The growth of CdS QDs was monitored via UV-visible spectra with the reaction time. After being refluxed at the 100 ^{0}C for 12 h the yellow, green QDs was removed from the mantle and cooled down to room temperature, then transferred to a conical flask and precipitated with acetone. This precipitate washed 3-4 times with acetone and dried to get crystalline powder. The purified crystalline powder used for the further studies.

The CdS QDs solutions with 1µM concentration were prepared by redispersing the CdS QDs powder in millipore water, and then different concentration of CTAB and SDS introduced in to the QDs solution to study the effect of surfactant on QDs stability and further growth.

CHARACTERIZATION

UV-Visible spectra were monitored using Thermoscintific evolution-300 spectrophotometer operated at a resolution of 2 nm. Fluorescence spectra were recorded using an Agilent fluorescence spectrophotometer (G9800AA). The FTIR spectra of thioglycolic acid and thioglycolic stabilized CdS quantum dots (TGA@CdS QDs) measured with Shimadju IR Affinity 8400S FTIR Spectrometer. TEM measurements performed on a JEOL, JEM-2100F, operated at accelerating voltage 200kV. SEM analysis has been carried out by ZEISS EVO (EVO 18) Series Scanning Electron Microscope. X-ray

diffraction study has been performed on PANalytical 3 kW X'pert Powder XRD – Multifunctional.

RESULTS AND DISCUSSION

Figure 1 A shows the representative set of refluxing time dependent (1-7 h) UV−vis spectra of TGA stabilized CdS QDs prepared using a Cd^{2+}: TU: TGA molar ratio of 1:2:3 and Cd^{2+} concentration of 5 mM. The absorption band of bulk CdS positioned at 515 nm [41]. Desired growth of CdS QDs achieved after 7 h refluxing. All samples showed well-defined first excitonic peaks between 330 to 392 nm with different refluxing time (Table 1) and attributed to 1sh-1se excitonic transitions [42]. These values signify that the shift in the absorption peak corresponding to the increase in particle diameter of the CdS QDs with the duration of the hydrothermal process.

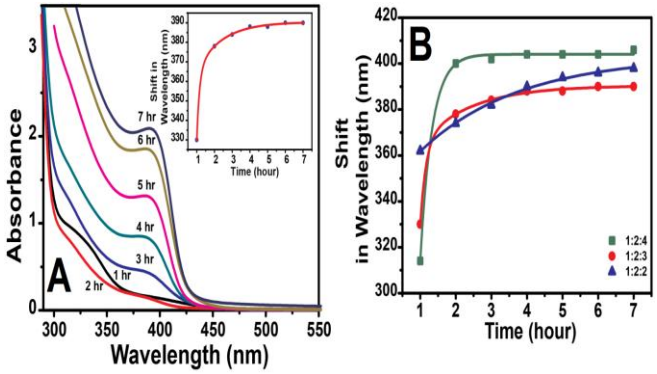

Figure 1. Absorption spectra of TGA stabilized CdS quantum dots with different time interval of refluxing time. Reaction Condition: (A) [$CdCl_2$. $5H_2O$] = 5mM [NH_2CSNH_2] = 10 mM [TGA] = 15 mM (B) Plot of shift in wavelength (λ_{max}) vs growth time.

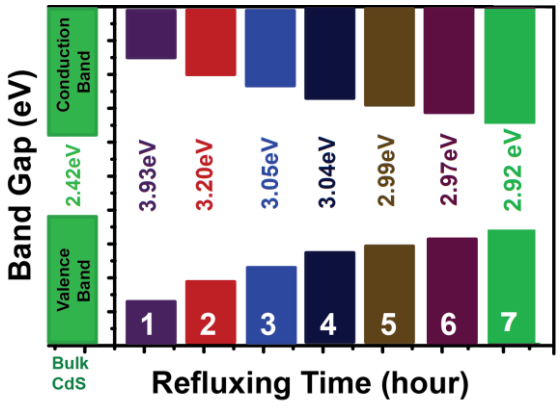

Figure 2. Cartoon representation of the variation of band gap with refluxing time.

Initially the absorption bands (t = 1 to 7 h) are broad; these broadness indicates the onset of conventional Ostwald ripening which causes a slow defocusing of size distribution [20]. Later on the bands become sharper as reaction time elapsed. The sharp absorption features are indicative of monodispersed particles. The variation of the absorption bands indicates that the particles grow rapidly as the reaction time increased. The corresponding absorption edges (obtained by the intersection of the sharply decreasing region of the spectrum with the baseline) [43] are located between 315 to 423 nm for reactions performed during 1 to7 h refluxing, which corresponds to band gaps of 3.93 to 2.92 eV, respectively (Figure 2). A comparison with the value of bulk CdS that have an absorption edge located at 515 nm (2.42 eV) indicates quantum confinement in all the sprepared nanocrystals. Using these band gap values, the particle diameters were calculated following the formula of Brus (Eq.1) based on the effective mass approximation [44–47],

$$E_{gn} = E_{gb} + \frac{h^2\pi^2}{2r^2}\left(\frac{1}{m_{ec}} + \frac{1}{m_{hv}}\right) - \frac{1.8e^2}{4\pi\varepsilon\varepsilon_o r} - \frac{0.12e^4}{h^2(4\pi\varepsilon\varepsilon_o)^2}\left(\frac{1}{m_{ec}} + \frac{1}{m_{hv}}\right)^{-1} \quad (1)$$

Eg is the band gap of the bulk material (2.42 eV), h is the reduced Plank's constant (6.58 × 10^{-16} eV), r is the radius of spherical nanocrystals, e is the charge of the electron (1.6 × 10^{-19} C), ε is the semiconductor dielectric constant (5.7), m_{ec} and m_{hv} are effective masses of the electrons and holes, respectively and m_o is the free electron mass (m_o = 9.11 × 10^{-28} g). With the effective masses of electrons (m_{ec} = 0.19m_o) and holes (m_{hv} = 0.8m_o), diameters of 1.5 to 4.1 ± 0.9 nm were found for CdS@TGA QDs obtained after 1 to 7 h reaction, respectively (Table 1). The deviation of 0.9 nm corresponds to ±10 nm for the determination of the absorption edges. The sizes of the CdS QDs were also estimated from the UV−vis absorption spectra by Peng's empirical equations [48, 49] and were found to be in good accordance with results obtained from the Brus formula (1.3 to 3.9 ± 0.9 nm for CdS@TGA QDs obtained after 1 to 7 h reaction, respectively). CdS QDs prepared by the organometallic TOP and TOPO based approach and its alternatives usually exhibit fluorescence emission dominated by the band-edge emission [48-55]. Generally, for CdS QDs with diameters ranging from 2.0 -5.3 nm, the PL emission is located between 375 and 460 nm [56].

Figure 3 shows fluorescence spectra of CdS@TGA quantum dots corresponding to the absorption spectra (Figure 1A). It is evident that the PL emission peak position varies with refluxing time from 511 to 598 nm (Table 1) in a similar manner as the absorption peak position and CdS QDs diameter varies. The considerable variation between the emission peak position and the absorption edge indicates that the present CdS QDs exhibit trap-state

emission rather than band-edge emission. The observed broad fluorescence peak is commonly attributed to the recombination of charge carriers trapped in the surface states and is related to the size of CdS QDs [56–59]. The smaller particles leads larger energy band gap, which in turn results more blue shift in fluorescence band. Fluorescence QYs of the samples have been determined using the fluorescein as fluorescence standard (94% QY in 0.1 M NaOH), reached up to 32% for the sample prepared during 7 h of refluxing and were independent of the excitation wavelength between 300 and 400 nm. PL QYs values increase continuously with increasing duration of refluxing time (12.5 - 32.5% (Table 1) for 1 to 7 h of refluxing, respectively). The increase in fluorescence QYs with nanocrystal growth of CdS QDs prepared via organometallic approach is recently reported [60]. In addition to this, it can also be observed that the full-width-at-half-maximum (FWHM) of fluorescence spectra is 147 to 119 nm, which is 4-5 times wider than the emission peaks of CdS QDs prepared in organic medium at elevated temperature [48-55]. This is the typical behavior of CdS QDs prepared via aqueous synthetic route. Furthermore, the fluorescence spectra (figure 3) is very fine, which indicates the particles with very less surface defects.

Table 1. Showing the variation of absorption and emission maxima, FWHM, quantum yield, band gap and size of the quantum dot at different reflux time.

λ_a = absorption maxima, λ_e = emission maxima, a* = Size calculated through brush equation for corresponding λ_a

Time (h)	λ_a(nm)	λ_e (nm)	FWHM (nm)	%QY	Band Gap(eV)	Size[a*] (nm)
1	330	511	147	12.5	3.93	1.5 ± 0.9
2	378	533	154	13.2	3.20	2.9 ± 0.9
3	384	556	149	14.1	3.05	3.4 ± 0.9
4	388	572	151	15.2	3.04	3.6 ± 0.9
5	388	577	130	20.0	2.99	3.8 ± 0.9
6	392	590	124	25.3	2.97	3.9 ± 0.9
7	392	598	119	32..5	2.92	4.1 ± 0.9

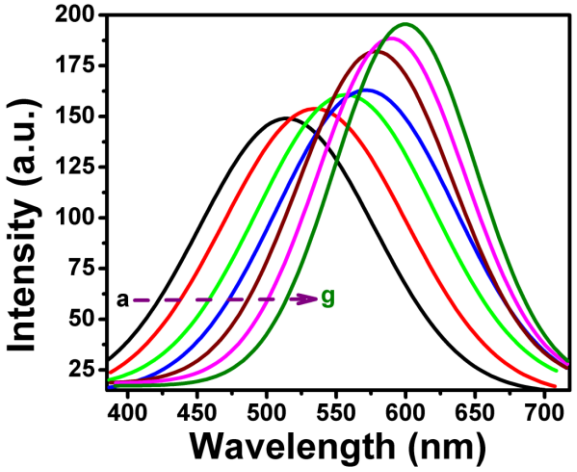

Figure 3. Fluorescence Spectra of TGA stabilized CdS quantum dots with different time interval of refluxing time. Reaction Condition: [$CdCl_2$. $5H_2O$] = 5mM. [NH_2CSNH_2] = 10 mM [TGA] = 15mM, pH = 10.5 Temp. 100 ^oC

Figure 1B shows the evolution of the first excitonic peak in absorption bands with growth for different molar ratio of Cd^{2+}: TGA from 1:2, 1:3, and 1:4. In these reactions, the Cd^{2+}: TU molar ratio kept constant at 1:2 and the variation in molar ratio of capping agent on growth kinetics has been studied. As can be seen, the variation of band position with refluxing time indicates the growth of the particle. The exponential growth of quantum dot has been observed with refluxing time, which seems that QDs growth follows first order kinetics. The first order rate constant for the growth of TGA@CdS QDs has been calculated using equation 2. The k_{obs} values for different molar ratio (Cd^{2+}: TGA) 1:2, 1:3, and 1:4 are $8.19x10^{-5}$ s^{-1}, $5.78x10^{-4}$ s^{-1}, and $2.21x10^{-4}$ s^{-1}, respectively. The k_{obs} value suggested that the particle growth rate is maximum at 1:3 of Cd^{2+} to TGA molar ratio.

$$k_{obs} = \frac{2.303}{t} log\frac{(\lambda_\infty - \lambda_0)}{(\lambda_\infty - \lambda_t)} \quad (2)$$

The increase in the ratio of TGA to Cd^{2+}: TU results the red shift of absorption and fluorescence spectra (Figure S1) which indicates the formation of larger CdS nanocrystallites with more surface defects than those prepared with smaller Cd^{2+}:TGA ratios (1:2 or 1:3). In the meantime, the fluorescence intensity showed a trend to increase first and decrease later, with maximum intensity at Cd^{2+}/TGA = 1:3. The fluorescence QYs of CdS@TGA QDs prepared with Cd^{2+}: TGA ratios of 1:2, 1:3, and 1:4 found to be 16.2, 32.0, and 5.04%, respectively. This behavior can be explained by the fact that increasing the amount of

TGA in solution leads to increasing TGA hydrolysis, and as a result, to a higher sulfide S^{2-} content in the reaction medium that accelerates the nanocrystals growth. It is also worthy to mention that for the lowest Cd^{2+}/TGA ratio (1:2), the dispersion stability was significantly lower and particles started to precipitate within one week. The reduced colloidal stability of these CdS@TGA QDs is probably an outcome of an incomplete surface passivation of the semiconductor dots. Considering the need for strong light intensity for bioapplications and bioimaging, 1:3 selected as the best Cd^{2+}: TGA ratio in this study.

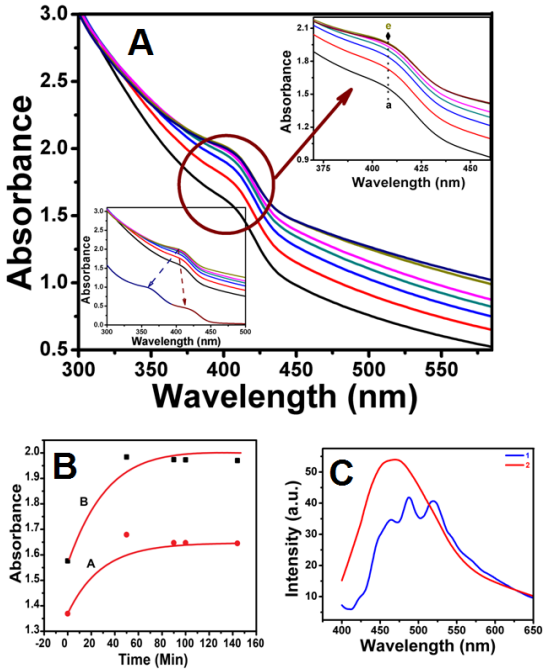

Figure 4. (A) Absorption spectra of CdS@TGA quantum dots in presence of 1mM CTAB (Inset Absorption spectra of CdS@TGA after a week) (B) plot of Absorbance Vs Time showing effect of CTAB on growth (C) fluorescence spectra of CdS@TGA quantum dots in presence of CTAB (1) just after the adding of CTAB (2) after a week.

Micellar arrangement can enhance the stability of QDs by preserving the nano-objects inside the micelle and promotes the monodispersity. Figure 4B shows the sequential set of UV-visible spectra of CTAB induced CdS@TGA QDs. These spectra suggested a growth pattern in the cationic micellar medium after introduction of CTAB in to the micromolar solution of CdS@TGA QDs. The absorption spectrum rises dramatically with a change in spectral pattern (Inset Figure 4) which indicates the micellar incorporation over CdS@TGA QDs. The growth pattern of CdS@TGA QDs with time for 2 different concentrations of CTAB over its CMC (1mM and 2mM) indicates that the [CTAB] is directly proportional to the growth rate (Figure 4B) (1.8x 10^{-3} s^{-1} in case of 2mM and 1.2 x 10^{-3} s^{-1} for 1mM surfactant concentration). The micelle induced evolution of 2 distinct absorption bands (Inset Figure 4A), one at shorter wavelength 350 nm and other at longer wavelength at 415 nm, indicates the formation of 2 different sized CdS QD which are well supported by the fluorescence spectra (Figure 4C).

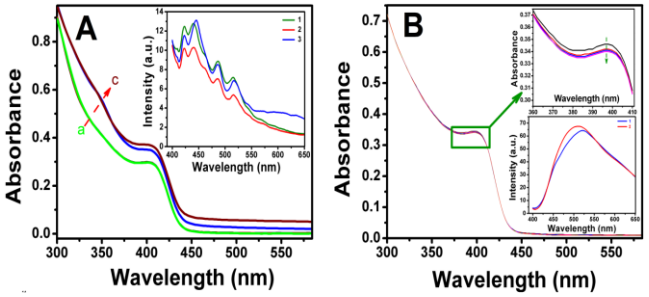

Figure 5. (A) Absorption spectra of CdS@TGA QDs in the presence of SDS (Inset fluorescence spectra of QDs in presence of SDS) (B) Absorption spectra showing the effect of Salt on the absorption spectral behavior of QDs (Inset: fluorescence spectra of CdS@TGA QDs dispersed in saline (1) just after the dispersion of QDs (2) after one week)

The CMC of SDS is found to be 6.39 mM under the reaction condition (Supporting information FigureS2). Therefore, a similar experiment was performed in the presence of 7 mM and 8.3 mM (CMC in aqueous medium) [61] SDS (Figure 5A and S2). We performed the above experiment at 7 mM as its CMC found to be decreased in presence of CdS@TGA QDs (Figure S2). No significant changes were observed as in case of CTAB. The reason might be the surface charge that QDs possess are negative ($-SCH_2CH_2COO^-$) which can be well counter controlled by cationic surfactants. Stability of CdS@TGA QDs against salt has been studied by exposing the CdS@TGA QDs to different concentration of NaCl as well with saline (Figure 5B). Negligible change observed in spectral behavior, even after one week and no sign of precipitation observed, which indicates the stability of CdS@TGA QDs in salt environment and is in good agreement with the PL emission spectrum (Inset of Figure 5B).

The FTIR spectra of thioglycolic acid and TGA-capped CdS QDs are shown in figure 6. The IR spectra of TGA-capped CdS QDs (red line) show significant changes as compared to thioglycolic acid (blue curve). The absence of stretching vibration of the thiol group (ν_{SH} = 2505cm^{-1}) in QD indicates thiolated interaction of TGA onto the QD surface. Furthermore, a significant shift in the asymmetric stretching vibration of the carboxyl group (ν_{COO}

=1700 cm^{-1} to 1585 cm^{-1}) also reveals thiolated interactions [62].

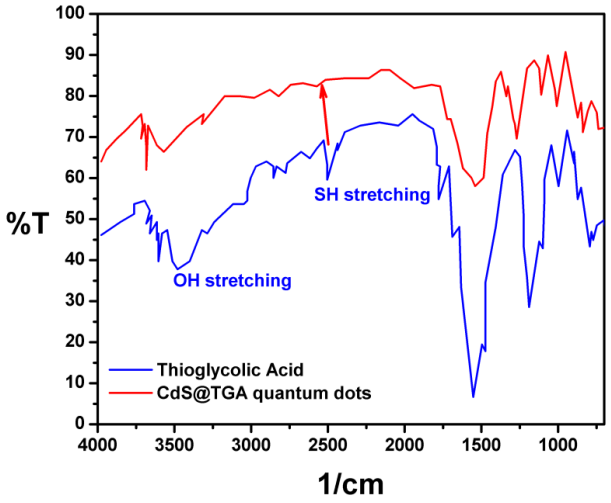

Figure 6. FTIR spectra of thioglycolic acid and TGA capped CdS QDs.

XRD and Electron Microscopic Analysis

Thioglycolic acid stabilized CdS (TGA@CdS) QDs were further characterized by X-ray powder diffraction (XRD) and transmission electron microscopy (TEM). Figure 7 shows the XRD pattern of CdS@TGA QDs of 2 different samples with different Cd^{2+} : TGA ratio. The broad peak indicates nano dimensions of the sample. With the increase in molar ratio, the peaks become more prominent and sharp due to the increase in nanocrystalline size. The less crystallinity observed in the sample prepared in 1:2 ratio, while higher crystallinity observed in 1:3 sample, which is in good agreement with the kinetic data. This significantly proves that higher growth rate produces higher crystalline material. The peaks are located at 2θ = 26.7, 43.8, and 51.3°, oriented along the (111), (220), and (311) directions are in good agreement with the JCPDS file 10−454 suggesting that the quantum dots are in cubic zinc blend form [63].

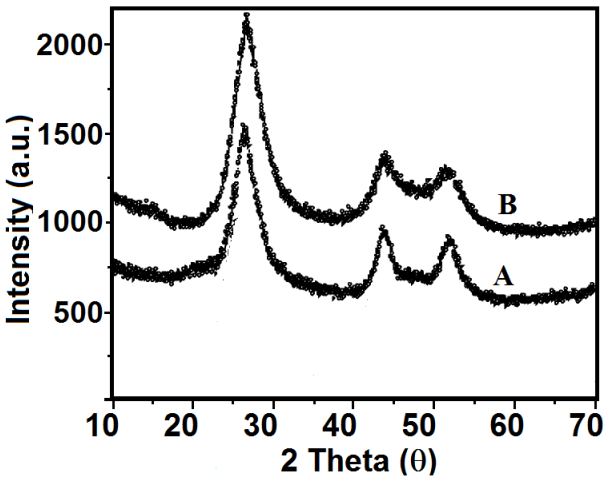

Figure 7. XRD of TGA stabilized CdS with (A) Cd:TGA ratio of 1:2 (B) Cd:TGA ratio of 1:3

Figure 8 represents TEM images of the CdS QDs prepared under optimized conditions, with Cd^{2+}: TGA 1:3. Insets of figure 8 show the corresponding selected area electron diffraction (SAED) pattern and frequency percentage of the CdS@TGA QDs. The images show that CdS@TGA QDs are spherical, well defined, and uniform in size and shape. The size distribution histogram for prepared nanocrystals suggested that the particles having size range 3-4 nm are present in large extent. The average sizes obtained from UV−visible spectra and TEM images resembles each other reasonably well. HR-TEM image of CdS@TGA QDs prepared after 7 h of refluxing illustrated, well-resolved lattice planes (Figure 8). From the lattice fringes of the micrograph, the interplanar spacing (d) was estimated to be 0.356 nm, which correlates to the miller indices (111) plane, i.e., 0.36 nm of the cubic phase. The cubic zinc blend structure of CdS nanoparticles was further evidenced by the SAED pattern. Scanning electron microscopic (SEM) image of CdS quantum dots shown in figure 8B reveals that CdS quantum dots are spherical in shape except few particles which are clumped together.

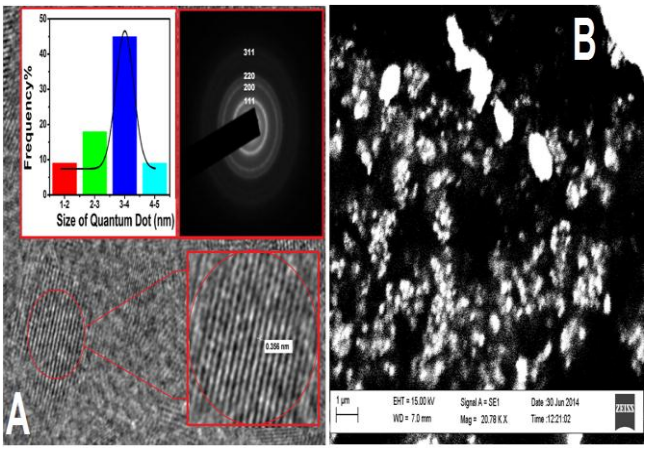

Figure 8. (A) HR-TEM image of CdS@TGA QDs (Inset: SAED pattern of CdS@TGA, Size distribution histogram) (B) SEM image of CdS@TGA quantum dots

CONCLUSION

CdS quantum dots were prepared through aqueous route with a cubic zinc blend structure using cadmium chloride and thiourea as cadmium and sulfur source and thioglycolic acid as a stabilizing agent. Effect of different molar ratio of Cd2+ to TGA were found to affect the growth kinetics of quantum dots, which was found to be 5.78x10-4 s-1 for the molar ratio 1:3. In optimal condition, the fluorescence spectra of CdS quantum dots ranges between 490 to 594 nm during 7 h of refluxing and the best fluorescence quantum yield reached up to 32%. The band gap of quantum dots found to be dependent on refluxing time and

varies from 3.93 eV to 2.92 eV. The evolution of two different absorption bands (350 and 418 nm) and emission peaks (470 and 540 nm) indicates bidispersity in the presence of CTAB. However, in case of SDS fluorescence peaks completely vanishes, without significant change in absorption spectra. Different concentration of salt showed an insignificant effect on QDs aggregation.

ACKNOWLEDGEMENT

Financial support from DST (New Delhi) Fast Track Project (SR/FT/CS-39/2011) New Delhi acknowledged with appreciation. We are thankful to sophisticated analytical instrument research facility (AIRF) Jawahar Lal Nehru University (JNU), New Delhi for TEM analysis. We are also grateful to head, School of Studies in Physics and Astrophysics, Pt. Ravishankar Shukla University, Raipur for FTIR analysis. Authors are thankful to the head, School of Studies in Chemistry, Pt. Ravishankar Shukla University, Raipur for providing laboratory facilities.

REFERENCES:

1. M. Kroutvar, V. Ducommun, D. Heiss, M. Bichler, D. Schuh, G. Abstreiter, J. J. Finley, Nature 2004, 432, 81.
2. X. Wu, H. Liu, J. Liu, K. N. Haley, J. A. Treadway, J. P. Larson, M. P. Bruchez, Nature Biotechnology 2002, 21, 41.
3. I. L. Medintz, H. T. Uyeda, E. R.Goldman, Nature Materials 2005, 4 , 435.
4. R. O. Moussodia, L. Balan, C. Merlin, C. Mustin, R. Schneider, J. Mater. Chem. 2010, 20, 1147.
5. F. Aldeek, C. Mustin, L. Balan, T. Roques-Carmes, M. P. Fontaine-Aupart, R. Schneider, Biomaterials 2011, 32, 5459.
6. F. Aldeek, R. Schneider, M. P. Fontaine-Aupart, C. Mustin, S. Lécart, C. Merlin, J. C. Appl. Environ. Micro. 2013, 79, 1400.
7. A. Aboulaich, L. Balan, J. Ghanbaja, G. Medjahdi, C. Merlin, R. Schneider, Chem. Mater. 2011,23, 3706.
8. B. Dong, L. Cao, G. Su, W. Liu, J. Phys. Chem. C 2012, 116, 12258.
9. K. Sooklal, B. S. Cullum, S. M. Angel, C. J. Murphy, J. Phys. Chem. 1996, 100 , 4551.
10. G. J. Ping, Y. D. Li, Adv. Funct. Mater. 2004, 14.2,157.
11. G. Shen, J. H. Cho, J. K. Yoo, G. C. Yi, C. J. Lee, J. Phys. Chem. B 2005, 109, 9294.
12. K. Yu, M. Z. Hu, R. Wang, M. L. Piolet, M. Frotey, M. B. Zaman, C. Li, J. Phys. Chem. C 2010, 114, 3329.
13. H. Li, W. Y. Shih, W. H. Shih, Ind. Eng. Chem. 2007, 46, 2013.
14. Z. Li, Y. Du, Mater. Lett. 2003, 57, 2480.
15. A. Mansur, H. Mansur, J. González, Sensors 2011, 11, 9951.
16. G. Mohammed, A. Abdul-Aziz, A. Bagabas, M. A. Dastageer, J. Nano. Res. 2011, 13.9, 3835.
17. Y. Wang, N. Herron, J. Phys. Chem. 1991, 94, 525.
18. W. W. Yu, E. Chang, R. Drezek, V. L. Colvin, Biochem. Biophys. Res. Commun. 2006, 348, 781.
19. K. E. Sapsford, T. Pons, I. L. Medintz, H. Mattoussi, Sensors 2006, 6, 925.
20. X. Zhong, R. Xie, Y. Zhang, T. Basché, W. Knoll, Chem. Mater. 2005, 17, 4038.
21. L. Liu, Q. Peng, Y. Li, Inorg. Chem. 2008, 47, 3182.
22. C. Dong, H. Qian, N. Fang, J. Ren, J. Phys. Chem. B 2006, 110,11069.
23. L. H. Hanus, K. Sooklal, C. J. Murphy, H. J. Ploehn, Langmuir 2000, 16, 2621.
24. J. O. Winter, N. Gomez, S. Gatzert, C. E. Schmidt, B. A. Korgel, Colloids Surf., A 2005, 254, 147.
25. H. Fan, E. W. Leve, C. Scullin, J. Gabaldon, D. Tallant, S. Bunge, C. J. Brinker, Nano Letters 2005, 5, 645.
26. J. Xiang, H. Cao, Q. Wu, S. Zhang, X. Zhang, Cryst. Growth Des. 2008, 8, 3935.
27. S. Chen, J. Zhu, Y. Shen, C. Hu, L. Chen, Langmuir 2007, 23, 850.

28. B. A. Kairdolf, A. M.Smith, S. Nie, J. Am. Chem. Soc. 2008, 130, 12866.

29. D. A. R. Barkhouse, A. G. Pattantyus-Abraham, L. Levina, E. H. Sargent, ACS Nano 2008, 2, 2356.

30. P. Thangadurai, S. Balaji, P. T. Manoharan, Nanotechnology 2008, 19, 435708.

31. N. Pradhan, S. Efrima, J. Am. Chem. Soc. 2003, 125, 2050.

32. Y. C. Cao, J. Wang, J. Am. Chem. Soc. 2004, 126,14336.

33. O. Chen, Y. Yang, T. Wang, H. Wu, C. Niu, J. Yang, Y. C. Cao, J. Chem. Soc. 2011, 133, 17504.

34. O. Chen, X. Chen, Y. Yang, J. Lynch, H. Wu, J. Zhuang, Y. C. Cao, Ang. Chem. Int. Ed. 2008, 47, 8638.

35. K. Yu, M. Z. Hu, R. Wang, M. L. Piolet, M. Frotey, M. B. Zaman, C. Li, J. Phys. Chem. C 2010, 114, 3329.

36. N. G. Piven, Y. B. Khalavka, L. P. Shcherbak, Inorg. Mater. 2008, 44, 1047.

37. J. E. Govan, E. Jan, A. Querejeta, N. A. Kotov, Y. K. Gunko, Chem. Commun. 2010, 46, 6072.

38. S. Karan, B. Malik, J. Phys. Chem. C 2007, 111, 16734.

39. J. Zhang, L. D. Sun, X. C. Jiang, C. S. Liao, C. H. Yan, Cryst. Growth Des. 2004, 4, 309.

40. B. A. Simmons, S. Li, V. T. John, G. L. McPherson, A. Bose, W. Zhou, J. He, Nano Letters 2002, 2, 263.

41. P. Mandal, S. S. Talwar, S. S. Major, R. S. Srinivasa, J. Chem. Phys. 2008, 128 , 114703.

42. W. T. Yao, S. H. Yu, S. J. Liu, J. P. Chen, X. M. Liu, F. Q. Li, J. Phys. Chem. B 2006, 110, 11704.

43. M. Moffitt, A. Eisenberg, Chem. Mater. 1995, 7, 1178.

44. L. Brus, J. Phys. Chem. 1986, 90, 2555.

45. Y. Wang, N. Herron, J. Phys. Chem. 1991, 95, 525.

46. A. Henglein, Chem. Rev. 1989, 89, 1861.

47. Y. D. Li, H. W. Liao, Y. Ding, Y. T. Qian, L. Yang, G. E. Zhou, Chem. Mater. 1998, 10, 2301.

48. I. Robel, M. Kuno, P. V. Kamat, J. Am. Chem. Soc. 2007, 129, 4136.

49. Y. Chen, K. Munechika, I. Jen-La Plante, A. M. Munro, S. E. Skrabalak, Y. Xia, D. S. Ginger, Appl. Phys. Letters 2008, 93, 53106.

50. W. W. Yu, X. Peng, Ang. Chem. Int. Ed. 2002, 41, 2368.

51. W. W. Yu, Y. A. Wang, X. Peng, Chem. Mater. 2003, 15, 4300.

52. D. Pan, S. Jiang, L. An, B. Jiang, Adv. Mater 2004, 16, 982.

53. Q. Wang, D. Pan, S. Jiang, X. Ji, L. An, B. Jiang, Chem. Euro. J. 2005, 11, 3843.

54. L. Zeiri, I. Patla, S. Acharya, Y. Golan, S. Efrima, J. Phys. Chem. C 2007, 111,11843.

55. Y. Miao, Z. Wu, L. Cao, L. Fu, Y. He, S. Xie, B. Zou, Opt. Mater. 2004, 26, 71.

56. C. H. Fischer, A. Henglein, J. Phys. Chem. 1989, 93, 5578.

57. H. Fujiwara, H. Hosakawa, K. Murakoshi, Y. Wada, S. Yanazida, T. Okada, H. Kobayashi, J. Phys. Chem. B 1997, 101, 8270.

58. L. Qi, H. Colfen, M. Antonietti, Nano Letters 2001, 1, 61.

59. C. Lu, B. Yang, J. Mater. Chem. 2009, 19, 2884.

60. H. L. Chou, C. H. Tseng, K. C. Pillai, B. J. Hwang, L.Y. Chen, Nanoscale 2010, 2, 2679.

61 A. Dominguez, A. Fernandez, N. Gonzalez, E. Iglesias, L. Montenegro, J. Chem. Edu. 1997, 74, 1227.

62. M. Y. Li, H. M. Zhou, H. Y. Zhang, P. Sun, K. Yi, M.Wang, Z. Dong, S. Xu, J. Lumin. 2010, 130, 1935.

63. A. Aboulaich, D. Billaud, M. Abyan, L. Balan, J. J. Gaumet, G. Medjadhi, J. Ghanbaja, R. Schneider, ACS Appl. Mater. Interfaces 2012, 4, 2561.